

This discussion paper is/has been under review for the journal Hydrology and Earth System Sciences (HESS). Please refer to the corresponding final paper in HESS if available.

Temporal stability of soil moisture under different land uses/cover in the Loess Plateau based on a finer spatiotemporal scale

J. Zhou, B. J. Fu, N. Lü, G. Y. Gao, Y. H. Lü, and S. Wang

State Key Laboratory of Urban and Regional Ecology, Research Center for Eco-Environmental Sciences, Chinese Academy of Sciences, P.O. Box 2871, Beijing 100085, China

Received: 5 July 2013 – Accepted: 21 July 2013 – Published: 6 August 2013

Correspondence to: B. J. Fu (bfu@rcees.ac.cn)

Published by Copernicus Publications on behalf of the European Geosciences Union.

HESSD
10, 10083–10125, 2013

Temporal stability of
soil moisture under
different land
uses/cover

J. Zhou et al.

[Title Page](#)
[Abstract](#) [Introduction](#)
[Conclusions](#) [References](#)
[Tables](#) [Figures](#)

[◀](#) [▶](#)
[◀](#) [▶](#)
[Back](#) [Close](#)
[Full Screen / Esc](#)

[Printer-friendly Version](#)
[Interactive Discussion](#)



Abstract

The Temporal stability of soil moisture (TSSM) is an important factor to evaluate the value of available water resources in a water-controlled ecosystem. In this study we used the evapotranspiration-TSSM (ET-TSSM) model and a new sampling design to examine the soil water dynamics and water balance of different land uses/cover types in a hilly landscape of the Loess Plateau under a finer spatiotemporal scale. Our primary focus is to examine the difference among soil water processes, including the wet-to-dry (WTD) process triggered by precipitation and the dry-to-wet (DTW) process caused by radiation among varied land uses/cover types. Three vegetation types and bare land were selected in the sampling scheme. For each land uses/cover type, four microplots (60cm × 60cm) were established, and the soil moisture was measured at the central point (CP) and four ambient points (AP). The results indicated that (1) the bare land (plot1) was sensitive to the influence of rainfall and radiation compared with other land uses types; (2) *Andropogon* (plot2) and *Spiraea pubescens* (plot4) more efficiently represented the average soil moisture of the different land uses/cover in the WTD and DTW processes, respectively, in the CP position. In contrast, the bare land and *Artemisia coparia* (plot3) seemed to be more representative of the average soil water content in the AP position; (3) the ET-TSSM model demonstrated that, in the WTD processes, although *Spiraea pubescens* land use reached the net deficit of the soil water storage condition was longest, the vegetated land uses have a higher capacity of water consumption than bare land and more easily affected the serious condition of the soil water deficiency at the end of WTD processes. We concluded that a finer spatiotemporal scale in the TSSM study could be a new method to describe the effect of plant on soil moisture dynamics triggered by precipitation or radiation and that the improvement of the application of the TSSM-based model to hydrological processes could be a promising research subject in the future.

Temporal stability of soil moisture under different land uses/cover

J. Zhou et al.

Title Page

Abstract

Introduction

Conclusion

References

Tables

Figures



Bac

Close

Full Screen / Esc

[Printer-friendly Version](#)

Interactive Discussion

1 Introduction

Soil moisture is one of indispensable stress factors to have a far-reaching effect on the hydrological process in water-controlled ecosystems (Noy-Meir, 1973). Especially in arid and semi-arid regions (e.g., the Loess Plateau, China), exploring the influence of the soil water on the hydrological cycle of the soil-plant-atmosphere continuum is crucial to the investigation into available water resources. As an exploratory method to describe the temporal distribution of the soil water content, the temporal stability of soil moisture (TSSM) was defined as the time invariant association between spatial location and statistical parametric values based on the probability density function of the soil water (Vachaud et al., 1985). The introduction of the TSSM concept into hydrological studies supplied a comprehensive understanding of the soil moisture dynamic change with different temporal scales, but it also likely offered a new method to evaluate and analyze the value of the soil moisture on water-limited ecosystems.

The TSSM was initially used to optimize uniform and sufficient spatial sampling points of the soil water content to reduce the level of uncertainty of the soil water distribution estimation at the watershed scale (Vachaud et al., 1985; Van Pelt and Wierenga, 2001). Therefore, coarser spatial scales of the TSSM studies were first systematically investigated. These ranged from multiple investigated fields scales (300 m^2 per field) (Brocca et al., 2010) to hillslope scales (approximate 900 m^2) (Coppola et al., 2011) or from watershed scales (610 km^2 and 1285 km^2 respectively) (Martinez-Fernandez and Ceballos, 2003; Starks et al., 2006) to landscape scale (Martinez-Fernandez and Ceballos, 2003). Based on the characteristics of the TSSM's response to coarser spatial scales, the topography (Brocca et al., 2009, 2007), soil texture (Cosh et al., 2006; Gao and Shao, 2012; Pachepsky et al., 2005; Starks et al., 2006), precipitation and vegetation type (Brocca et al., 2009; Jia and Shao, 2013; Mohanty and Skaggs, 2001) were summarized as the main influencing factors of the TSSM.

Second, the integration of the TSSM and mathematical statistics method became the main application of the TSSM to calibrate the accuracy of soil moisture remote sensing

[Title Page](#)[Abstract](#)[Introduction](#)[Conclusions](#)[References](#)[Tables](#)[Figures](#)[◀](#)[▶](#)[◀](#)[▶](#)[Back](#)[Close](#)[Full Screen / Esc](#)[Printer-friendly Version](#)[Interactive Discussion](#)

data in large spatial scales. Combining the TSSM with a remote sensing technique (Jacobs, 2004; Martinez-Fernandez and Ceballos, 2003; Mohanty and Skaggs, 2001) effectively promoted the precision of the soil moisture estimation, and the introduction of other mathematical analysis tools – the geostatistical method (Brocca et al., 2009),
5 spatial autocorrelation technique (Coppola et al., 2011) and wavelet coherency analysis algorithm (Biswas and Si, 2011) – into the TSSM concept also further expanded its applicability to estimate the soil moisture distribution.

To summarize, three elements, including a uniform sampling strategy, coarser spatial scale and aim to improve soil water estimation, constituted the fundamental analysis methodology and main application of former TSSM studies, and they also supplemented the temporal characteristics of the available soil water resources with spatial-based ecohydrological studies in a water-limited ecosystem. However, the coarser spatial scale of the TSSM investigation likely neglected some important temporal information of the soil moisture existing at finer spatial scales (e.g., single-plant scale). Nevertheless,
10 the TSSM at the single-plant scale could reflect the characteristics of the water dynamic mechanisms operating in the soil and plant environments with time. In practical terms, comprehensively understanding these mechanisms was greatly significant for the strategy of vegetation layout in water-controlled ecosystems, and from a theoretical view, exploring the causes of these mechanisms has become a challenging issue for certain related interdisciplinary research fields (Newman et al., 2006).

In addition to downscaling the coarser spatial scale to a finer scale, if we applied the TSSM's features in the finer scale with different land uses to the corresponding hydrological process analysis, a new method to assess the water conservation or loss effect taken by the various plants or land cover in terms of evaluating the corresponding
15 temporal fluctuation of the soil moisture, could be supplied or could provide additional parameters for some process-based hydrological models to interpret the role played by plants in the water cycle in arid and semi-arid areas. Consequently, a new experimental design that was distinct from uniform sampling was also needed, because the soil moisture sampling design should be appropriate for both the interspersion of a finer

[Title Page](#)

[Abstract](#)

[Introduction](#)

[Conclusions](#)

[References](#)

[Tables](#)

[Figures](#)

◀

▶

◀

▶

[Back](#)

[Close](#)

[Full Screen / Esc](#)

[Printer-friendly Version](#)

[Interactive Discussion](#)

spatial scale and the observation of hydrological processes in different land uses. In conclusion, three elements being different from former TSSM studies constituted the main study framework in this paper. They were hydrological-based sampling strategy, finer spatial scale of different land uses/cover and the purpose of exploring the new method to analyze hydrological processes through TSSM characteristics.

Specifically, as our study region, the Loess Plateau was an ideal experimental environment (Chen et al., 2010; Gao et al., 2011; Qiu et al., 2001; Wang et al., 2013) in which the spatiotemporal variability of soil moisture has been extensively studied (Shao et al., 2010; Tian and Peng, 1994). The previous TSSM studies mainly concentrated on the characteristics of the TSSM of the main vegetation types, including grassland, shrubland and other land uses at the watershed scale (Gao and Shao, 2012; Hu et al., 2010; Jia and Shao, 2013). However, the characteristics of the TSSM of other vegetation types at finer spatial scales have been less studied. In this paper, we selected 12 typical vegetation microplots and 4 bare microplots distributed on a specific hillslope randomly as research objects. Employing a soil water sampling scheme that combined the TSSM with specific hydrological responses, we compared the TSSM of the bare patch with that of vegetation, and analyzed the probable influencing factors of the TSSM under the finer spatial scale condition. Our objective was to explore a new method to evaluate the ecohydrological effect of different land uses/cover in the Loess Plateau.

2 Material and methods

2.1 Description of study area

The experiment was conducted in the Yangjuangou Catchment ($36^{\circ}42' N$, $109^{\circ}31' E$, 2.02 km^2) which is located in the central part of the Loess Plateau (Fig. 1a). The elevation of the Yangjuangou Catchment ranges from 1050 m to 1298 m, and its slope gradients mainly change between 17.6 % and 57.7 % (Liu et al., 2012). Its climate is primarily

[Title Page](#)

[Abstract](#)

[Introduction](#)

[Conclusions](#)

[References](#)

[Tables](#)

[Figures](#)

◀

▶

◀

▶

[Back](#)

[Close](#)

[Full Screen / Esc](#)

[Printer-friendly Version](#)

[Interactive Discussion](#)



influenced by the North China monsoon. The precipitation displaying significant inter-annually variability (Liu et al., 2012) mainly occurs between June and September and totals approximately 535 mm per year (Gao et al., 2012). Loessal soil was the main soil type in the Yangjuangou catchment, it has a weak structure and high erosional sensitivity to water (Gao et al., 2012; Li et al., 2003; Wang et al., 2009). The dominant vegetation types include *Stipa bungeana* (*Andropogon*), *Hippophae rhamnoides*, *Artemisia scoparia*, *Piraea pubescens* and *Prunus armeniaca* var. *ansu* (Shao et al., 2010). Due to the wide implementation of the Grain-for-Green program in the Loess Plateau since 1998, the Yangjuangou Catchment was also planted with a large amount of artificial vegetation – such as *Robinia pseudoacacia* Linn, *Platycladus orientalis*, *Lespedeza davurica*, and *Amorpha fruticosa*.

2.2 CP/APs sampling schemes

We designed 16 microplots (60 cm × 60 cm each) representing 4 different land uses/cover which include bare land cover (plot1), *Andropogon* (plot2), *Artemisia coparia* (plot3), and *Spiraea pubescens* (plot4) (Table 1). All of the plots are distributed along one southwest–northeast aspect hillslope located in the middle part of the catchment (Fig. 1b). The sampling points of the soil moisture in all microplots were arranged in terms of two types: (1) a central point (CP) per plot, which was mainly sited on or near the base of each vegetated microplot (plot3 and 4) or in the middle of the other microplots (plot1 and 2); and (2) 4 ambient points (APs) per plot, which were located the CP (Fig. 1b). The purpose of applying the CP/APs sampling scheme was primarily depended on the different soil moisture plus (Rodríguez-Iturbe et al., 2001) that likely existed in the heterogeneous vegetation with an obvious diversity of morphological features. In fact, a single plant could be regarded as a collection of precipitation in water-controlled ecosystems by means of stemflow systems (Li, 2011), which most likely affect the hydrological processes of soil. Therefore, the CP sampling scheme was planned to analyze the soil moisture dynamics in the middle points receiving the stemflow generated in different canopy structures of vegetated microplots during

Temporal stability of soil moisture under different land uses/cover

J. Zhou et al.

[Title Page](#)

[Abstract](#)

[Introduction](#)

[Conclusions](#)

[References](#)

[Tables](#)

[Figures](#)

◀

▶

◀

▶

[Back](#)

[Close](#)

[Full Screen / Esc](#)

[Printer-friendly Version](#)

[Interactive Discussion](#)



precipitation processes, and the aim of the AP sampling scheme was to investigate the change in the soil water content in the surrounding points that are likely affected by the throughfall as a result of the precipitation intercepted by the canopy structure. Moreover, employing the CP/APs sampling scheme likely also indicated the soil moisture loss of different points during evapotranspiration processes. We employed the Field-Scout TDR 300 Soil Moisture Meter (Spectrum Technologies, Inc, Aurora, Illinois, USA) to measure the soil moisture of the 0 ~ 10 cm depth layer of every CP and AP from the 8 August 2012 to 20 September 2012 resulting in 960 soil moisture records. Furthermore, we carefully mended the disturbed holes after every measurement by the TDR to reduce the system error derived from the inevitable disturbance of the soil surface layer.

2.3 Quantification of TSSM

2.3.1 Mean relative difference (MRD) of the TSSM (TSSM-MRD)

The MRD of the soil moisture indicates the fluctuation of every measuring point compared with the average value over a specific observation period (Vachaud et al., 1985). With respect to the CP sampling scheme, the MRD calculation was performed as follows:

$$\Delta_{CP(i,j)} = \theta_{CP(i,j)} - \bar{\theta}_{CP(j)} \quad (1)$$

$$\bar{\theta}_{CP(j)} = (1/16) \sum_{i=1}^{16} \theta_{CP(i,j)} \quad (2)$$

$$\delta_{CP(i,j)} = \Delta_{CP(i,j)} / \bar{\theta}_{CP(j)} \quad (3)$$

where $\theta_{CP(i,j)}$ is the soil moisture of the CP on the i th microplot ($i = 1 \sim 16$) at j th observation time ($j = 1 \sim n$ which is concentrated at the special period) and $\bar{\theta}_{CP(j)}$ represents the average soil moisture of the CP in all microplots at the j th time. Therefore,

[Title Page](#)

[Abstract](#)

[Introduction](#)

[Conclusions](#)

[References](#)

[Tables](#)

[Figures](#)

[◀](#)

[▶](#)

[◀](#)

[▶](#)

[Back](#)

[Close](#)

[Full Screen / Esc](#)

[Printer-friendly Version](#)

[Interactive Discussion](#)

[Title Page](#)[Abstract](#)[Introduction](#)[Conclusions](#)[References](#)[Tables](#)[Figures](#)[◀](#)[▶](#)[◀](#)[▶](#)[Back](#)[Close](#)[Full Screen / Esc](#)[Printer-friendly Version](#)[Interactive Discussion](#)

$\Delta_{CP(i,j)}$ reflects the fluctuation of the soil moisture at location i at time j , and $\delta_{CP(i,j)}$ represents the relative soil moisture in the CP.

With respect to the APs, the MRD calculation was performed as follows:

$$\Delta_{AP(i,j)} = \bar{\theta}_{AP(i,j)} - \bar{\bar{\theta}}_{AP(j)} \quad (4)$$

$$\bar{\theta}_{AP(i,j)} = (1/4) \sum_{p=1}^4 \theta_{AP(i,j,p)} \quad (5)$$

$$\bar{\bar{\theta}}_{AP(j)} = (1/16) \sum_{i=1}^{16} \bar{\theta}_{AP(i,j)} = (1/64) \sum_{i=1}^{16} \sum_{p=1}^4 \theta_{AP(i,j,p)} \quad (6)$$

Therefore, Eqs. (4)–(6) corresponds to the relative difference of the APs:

$$\delta_{AP(i,j)} = \Delta_{AP(i,j)} / \bar{\bar{\theta}}_{AP(j)} \quad (7)$$

- where $\bar{\theta}_{AP(i,j)}$ is the average soil moisture of the 4 APs located in different positions (short for p) on the i th microplot at the j th time and the average soil moisture of all the different land-uses located in the APs at the j th time is displayed as $\bar{\bar{\theta}}_{AP(j)}$ by replacing the 4 APs' soil moisture with the mean value in every microplot.

Finally, the MRD ($\delta_{CP(j)}$, $\delta_{AP(j)}$) and standard deviation ($\varsigma(\bar{\delta}_{CP(j)})$ and $\varsigma(\bar{\delta}_{AP(j)})$) of the CP and APs, respectively, are determined in Eqs. (8)–(11) respectively.

$$\bar{\delta}_{CP(j)} = (1/n) \sum_{j=1}^n \delta_{CP(i,j)} = (1/n) \sum_{j=1}^n \left(\frac{16\theta_{CP(i,j)} - \sum_{i=1}^{16} \theta_{CP(i,j)}}{\sum_{i=1}^{16} \theta_{CP(i,j)}} \right) \quad (8)$$

$$\varsigma(\bar{\delta}_{CP(j)}) = \sqrt{\sum_{j=1}^n \frac{(\delta_{CP(i,j)} - \bar{\delta}_{CP(j)})^2}{6}} \quad (9)$$

and

$$\bar{\delta}_{AP(j)} = (1/n) \sum_{j=1}^n \delta_{AP(i,j)} = (1/n) \sum_{j=1}^n \left(\frac{16 \sum_{p=1}^4 \theta_{AP(i,j,p)} - \sum_{i=1}^{16} \sum_{p=1}^4 \theta_{AP(i,j,p)}}{\sum_{i=1}^{16} \sum_{p=1}^4 \theta_{AP(i,j,p)}} \right) \quad (10)$$

$$\zeta(\bar{\delta}_{AP(j)}) = \sqrt{\sum_{j=1}^n \frac{(\delta_{AP(i,j)} - \bar{\delta}_{AP(j)})^2}{6}} \quad (11)$$

- Moreover, the MRD represents whether the value of the soil moisture in a given specific microplot overestimates ($\bar{\delta}_j > 0$) or underestimates ($\bar{\delta}_j < 0$) (Vachaud et al., 1985) the average soil moisture of all microplots over a specific period. Its standard deviation determines the fluctuation of the soil moisture at a given position of some microplots during the experiments. A given microplot is considered to better represent the TSSM during the observation process (Starks et al., 2006) when its $\zeta(\bar{\delta}_j)$ is smaller. Therefore, the TSSM-MRD could be regarded as the dominant standard to describe the characteristics of the TSSM under different land uses/cover.

2.3.2 Cumulative Probability (CumuP) of the soil moisture

- In contrast to the TSSM-MRD, which describes the dynamic characteristics of the TSSM, the CumuP of the soil water content represents a static feature of the TSSM. The CumuP calculation in the CP can be used as an example.

$$\bar{\theta}_{CP(i)} = (1/n) \sum_{j=1}^n \theta_{CP(i,j)} \quad (12)$$

where $\bar{\theta}_{CP(i)}$ is the average soil moisture of the i th microplot ($i = 1 \sim 16$) over n times during the specific experimental period. Then, all the different values of $\bar{\theta}_{CP(i)}$ should be

[Title Page](#)

[Abstract](#)

[Introduction](#)

[Conclusions](#)

[References](#)

[Tables](#)

[Figures](#)

◀

▶

◀

▶

[Back](#)

[Close](#)

[Full Screen / Esc](#)

[Printer-friendly Version](#)

[Interactive Discussion](#)

ranked from lowest to highest, such as $\bar{\theta}_{CP[1]} \leq \bar{\theta}_{CP[2]} \cdots \leq \bar{\theta}_{CP[16]}$ in which the number in the square bracket indicates the order of the average soil moisture. Additionally, the average soil moisture of all microplots over n times is expressed by Eq. (13):

$$\theta_{CP(i)} = \sum_{i=1}^{16} \bar{\theta}_{CP(i)} = (1/n) \sum_{j=1}^n \sum_{i=1}^{16} \theta_{CP(i,j)} \quad (13)$$

- 5 Therefore, the probability of lowest average soil moisture of some microplots over n observational times, $p(\bar{\theta}_{CP[1]})$ could be calculated by Eq. (14):

$$p(\bar{\theta}_{CP[1]}) = \bar{\theta}_{CP[1]} / \theta_{CP(i)}; \quad p(\bar{\theta}_{CP[1]}) \in (0, 1] \quad (14)$$

Based on this equation, the CumuP of the k th highest soil moisture of a microplot, CumuP($\theta_{CP[k]}$), could be expressed by Eq. (15):

$$10 \quad \text{CumuP}(\theta_{CP[k]}) = \sum_{k=1}^k p(\theta_{CP[k]}) \quad (15)$$

2.4 Evapotranspiration-TSSM (ET-TSSM) model

2.4.1 The selection of the parameter of TSSM (θ_s)

The hydrological response process of the soil moisture mainly consists of two components (Eagleson, 1978a), the soil water consumption process, which could be regarded as the change in the soil moisture condition from wet to dry (WTD), and the conservation process, which could be regarded as the shift in the soil moisture condition from dry to wet (DTW). Therefore, in this study, the two fundamental processes were introduced into the application of the TSSM in different land uses. We selected the parameters of the TSSM's application that met three requirements. First, in the WTD and

[Title Page](#)[Abstract](#)[Introduction](#)[Conclusions](#)[References](#)[Tables](#)[Figures](#)[◀](#)[▶](#)[◀](#)[▶](#)[Back](#)[Close](#)[Full Screen / Esc](#)[Printer-friendly Version](#)[Interactive Discussion](#)

DTW processes, the soil moisture in identical microplots has a similar CumuP rank, which means, specifically, that the difference between the CumuP of the soil moisture in same microplot was less than 0.1 between the two processes. Second, after meeting the first requirement, the CumuP should be closer to 0.5 representing the mean soil water content of all land uses/cover for both the WTD and DTW processes. Third, the same microplot should have the same rank in the MRD, and the absolute values of the MRD and standard deviation of the soil moisture in the same-rank microplot should both be as low as possible. All three requirements were the standards for the selection of the parameters of TSSM (θ_S), theoretically, not only perfectly quantified the TSSM characteristics of all land uses/cover, but also indicated the least fluctuation over the whole experimental period.

2.4.2 The framework of ET-TSSM models

A series of derivative parameters could be used to describe the hydrological response of different land uses/cover to the soil moisture pulse in WTD processes by the ET-TSSM model (Fig. 2). Primarily, we fitted some evapotranspiration curves (ET curves) based on the relationships between time (t) and soil moisture (θ).

$$\theta = \theta_n(t) \quad (16)$$

where $n = 1 \sim 4$ represents the 4 different land uses/cover in the Yangjuangou Catchment. In addition, we confirmed three ET-TSSM parameters from beginning (t_0) to end ($t_{e(n)}$), which characterized the application of TSSM to the hydrological processes.

WP_n parameter

If given soil moisture $\theta \in [\theta_S, \theta_n(t_0)]$, then:

$$WP_n = \int_{t_0}^{t_{s(n)}} \theta_n(t) dt - \theta_S(t_{s(n)} - t_0) \quad (17)$$

[Title Page](#)

[Abstract](#)

[Introduction](#)

[Conclusions](#)

[References](#)

[Tables](#)

[Figures](#)

[◀](#)

[▶](#)

[◀](#)

[▶](#)

[Back](#)

[Close](#)

[Full Screen / Esc](#)

[Printer-friendly Version](#)

[Interactive Discussion](#)

with

$$t_{s(n)} = \theta_n^{-1}(\theta_S) \quad (18)$$

where $t_{s(n)}$ expressed by the value of the inverse function $\theta_n^{-1}(x)$, represents the times at which the soil moisture of the 4 land uses/cover are on the threshold of the temporal stability condition during the WTD process, and also reflects how quickly the TSSM reached its threshold, which was influenced by the four different land uses/cover. And the WP_n means the cumulative effect of the soil moisture on the WTD processes, and reflects the possibility that the soil water storage of a specific land uses/cover is under the “water profit” condition before the soil water reached the threshold of the temporal stability condition $t_{s(n)}$ under different land uses/cover, and it also describes the capabilities of the different land uses/cover's with respect to water conservation during the decrease in moisture triggered by the radiation.

WD_n parameter

If $\theta \in (\theta_n(t_{e(n)}), \theta_S)$ then:

$$WD_n = \theta_s(t_{e(n)} - t_{s(n)}) - \int_{t_{s(n)}}^{t_{e(n)}} \theta_n(t) dt \quad (19)$$

$t_{e(n)}$ is the time at the end of the WTD process, and WD_n represents the cumulative effect of the soil moisture on time. However, this parameter indicates the “water deficit” condition after the soil water reached the threshold of the temporal stability condition $t_{s(n)}$, which also reflects the ability of the soil to lose water under different land uses/cover.

[Title Page](#)

[Abstract](#)

[Introduction](#)

[Conclusions](#)

[References](#)

[Tables](#)

[Figures](#)

[◀](#)

[▶](#)

[◀](#)

[▶](#)

[Back](#)

[Close](#)

[Full Screen / Esc](#)

[Printer-friendly Version](#)

[Interactive Discussion](#)

[Title Page](#)[Abstract](#)[Introduction](#)[Conclusions](#)[References](#)[Tables](#)[Figures](#)[◀](#)[▶](#)[◀](#)[▶](#)[Back](#)[Close](#)[Full Screen / Esc](#)[Printer-friendly Version](#)[Interactive Discussion](#)

$\Delta\theta_n$ parameter

Using Eq. (17) to subtract Eq. (19) yields:

$$\Delta\theta_n = WP_n - WD_n = \int_{t_0}^{t_{e(n)}} \theta_n(t)dt + \theta_S(t_0 - t_{e(n)}) = \int_0^{t_{e(n)}} \theta_n(t)dt - \theta_S t_{e(n)} \quad (20)$$

which means the dynamic changes in the water storage deviated by the TSSM parameter over a period lasting $t_{e(n)}$. Moreover if $t = t_{c(n)} = \theta_n^{-1}(\theta_{c(n)})$ and corresponding $\theta_{c(n)} = \theta_n(t_{c(n)})$, then $\Delta\theta_n = 0$.

With

$$\int_{t_0}^{t_{s(n)}} \theta_n(t)dt - \theta_S(t_{s(n)} - t_0) = \theta_S(t_{c(n)} - t_{s(n)}) - \int_{t_{s(n)}}^{t_{c(n)}} \theta_n(t)dt \quad (21)$$

Then we defined the $t_{c(n)}$ and $\theta_{c(n)}$ as the temporal threshold of the soil water storage balance and threshold of the soil water storage balance in different land uses respectively. Moreover, if $\theta_{c(n)} \in (\theta_n(t_{e(n)}), \theta_S)$ and $t_{c(n)} \in (t_{s(n)}, t_{e(n)})$. Then the piecewise Eq. (22) exists to describe the water balance based on the ET-TSSM model

$$\Delta\theta_n = \int_{t_0}^{t_{s(n)}} \theta_n(t)dt + \theta_S(t_0 - t) + \int_{t_{s(n)}}^t \theta_n(t)dt \begin{cases} > 0 & \theta \in (\theta_{c(n)}, \theta_S) & t \in (t_{s(n)}, t_{c(n)}) \\ = 0 & \theta = \theta_{c(n)} & t = t_{c(n)} \\ < 0 & \theta \in (\theta_n(t_{e(n)}), \theta_{c(n)}) & t \in (t_{c(n)}, t_{e(n)}) \end{cases} \quad (22)$$

Specifically, $\Delta\theta_n > 0$ and $\Delta\theta_n < 0$, in the sense of the TSSM, likely indicated that the soil water storage was under relatively sufficient and insufficient condition respectively at the end of the WTD process. Therefore, WP_n , WD_n , $\Delta\theta_n$, $t_{s(n)}$, $t_{c(n)}$ and $\theta_{c(n)}$ were the important parameters to integrate the TSSM with its application to the evaluation of hydrological processes in different land uses/cover.

3 Results

3.1 Hydrological responses of different land uses/cover

In the rainy season of 2012, the bare land cover appeared to be more sensitive to the influence of rainfall and radiation, having the largest magnitude of soil moisture dynamics (from $12.0\% \pm 1.01\%$ to $26.35\% \pm 1.51\%$). In contrast, the hydrological responses of *Andropogon* to the two triggers were the least obvious, with the mean soil moisture ranging from $10.9\% \pm 1.51\%$ to $22.4\% \pm 1.16\%$ (Fig. 3). Specifically, during the DTW processes, soil moisture of all plots displayed similar fluctuating trends (Fig. 4), but at the end of the DTW process, the average soil moisture of the bare land cover increased to the highest value in the CP (26.7%) and AP (26.0%) position. In addition, *Spiraea pubescens* reached the second highest value (24.6%) in the CP but seemed to be the least sensitive to the precipitation in the AP position. Otherwise, at the beginning of WTD process, the soil moisture of all land uses/cover in the CP position decreased by more significant levels, with magnitudes of 6.9% (bare land cover), 6.1% (*Andropogon*), 5.4% (*Artemisia coparia*), and 2.0% (*Spiraea pubescens*) respectively. However in the AP position, all the vegetated plots declined to a relatively similar level at the same time. But, according to the significant difference analysis, in both the WTD and DTW processes, the soil moisture of the different land uses/cover at the same sampling position showed no significant difference, and the soil moisture in the same land uses/cover at different sampling positions also showed no significant difference.

3.2 The TSSM of different land uses/cover

3.2.1 CP sampling-based TSSM (CP-TSSM) in hydrological processes

The MRD and CumuP determined the characteristics of the CP-TSSM. In the DTW process, the soil moisture in some of the *Andropogon* and *Spiraea pubescens* microplots most likely more efficiently represented the average soil moisture in the different land

[Title Page](#)

[Abstract](#)

[Introduction](#)

[Conclusions](#)

[References](#)

[Tables](#)

[Figures](#)



[Back](#)

[Close](#)

[Full Screen / Esc](#)

[Printer-friendly Version](#)

[Interactive Discussion](#)

Temporal stability of soil moisture under different land uses/cover

J. Zhou et al.

[Title Page](#)

[Abstract](#)

[Introduction](#)

[Conclusions](#)

[References](#)

[Tables](#)

[Figures](#)

[◀](#)

[▶](#)

[◀](#)

[▶](#)

[Back](#)

[Close](#)

[Full Screen / Esc](#)

[Printer-friendly Version](#)

[Interactive Discussion](#)



uses, with their CumuP being close to 0.5. With respect to the MRD, the soil moisture of the vegetated land uses tended to underestimate the mean soil water content due to their MRD values being larger than zero. *Spiraea pubescens*, with a mean standard deviation for CP of 0.134, could be regarded as the land uses with the least soil moisture fluctuation triggered by precipitation. In the WTD process, some *Andropogon* and *Artemisia coparia* plots with CumuP values of 0.47 and 0.53 respectively, could be more representative of the soil moisture in all land uses/cover. The MRD demonstrated that the soil water content in the bare land cover at the CP position was overestimated. *Spiraea pubescens* with a larger standard deviation (0.162) most likely had more obvious soil moisture fluctuations during the WTD process (Figs. 5 and 6).

3.2.2 AP sampling-based TSSM (AP-TSSM) in hydrological processes

With respect to the AP-TSSM, in the DTW process, the soil moisture of *Artemisia coparia* was overestimated, with its MRD being larger than zero. The CumuP of a few bare land covers and *Artemisia coparia* plots reached to 0.46 and 0.53 respectively, indicating that they were more representative of the average soil water content than the other two land uses. However, *Artemisia coparia* with the highest standard deviation of 0.089 revealed the largest magnitude of the soil moisture fluctuation. Otherwise, in the WTD process, two *Andropogon* microplots could represent the mean soil moisture in the AP position for all land uses/cover, and the soil moisture in the *Artemisia coparia* and *Spiraea pubescens* plots likely underestimated the average soil moisture of the different land uses/cover. Moreover, the soil water content in the bare land cover displayed a stronger temporal stability during the WTD process due to its lowest standard deviation value (0.074) (Figs. 7 and 8).

3.2.3 The determination of θ_S in two processes

Based on the integration of the principle of θ_S selection with the CP/AP sampling schemes both mentioned in the methods (Table 2), the results (Table 3) showed that, in

the CP position, plot4(3) (*Spiraea pubescens*) with MRD values of -0.034 and -0.004 in DTW and WTD process respectively, and a CumuP value of 0.59 in both, was selected as θ_S ; in the AP position, plot3(2) (*Artemisia coparia*) with 0.04 and -0.005 as the MRD of the soil moisture in the DTW and WTD processes respectively, and low standard deviations (0.028 and 0.055 respectively) was selected as θ_S . Consequently, plot4(3) and plot3(2) which had an average soil moisture in the WTD process of approximately 16.6% and 16.4% , respectively, were determined to represent the θ_S in the CP and AP sampling schemes, respectively.

3.3 TSSM's application on hydrological processes

- 10 The relationship between θ_S and the ET function is shown in Fig. 9. First, from the soil water storage view, at the CP position, WP_n in *Spiraea pubescens* and *Andropogon* reached the largest (290.93) and smallest (61.58) values, respectively. Then, at the end of the WTD process ($t_{e(n)} = 288$ h), WD_n was lower in the bare land cover (743.63) than in the other plots. Furthermore, the soil water storage in all the microplots was most likely under the insufficient conditions ($\Delta\theta_n < 0$). However, the extent of the water deficiency in the vegetated land uses was more obvious than in the bare land cover. With respect to the AP sampling schemes, *Artemisia coparia*, with a WP_n of 186.96 appeared to have more sufficient soil water storage than the other two vegetated plots. As the soil moisture continued to decrease, the soil moisture storage of $Artemisia coparia$ and the bare land cover represented the most ($WD_n = 1083.39$) and least ($WD_n = 697.09$) significant deficit situations respectively. Moreover, at the end of the WTD process, the bare land cover had the highest soil moisture shortage in both the AP and CP positions, with its $\Delta\theta_n$ being largest among all the plots (Table 4). From the temporal threshold of the soil water storage balance ($t_{c(n)}$) view, all of the $t_{c(n)}$ in the different land uses/cover met the condition $-t_{c(n)} \in (t_{s(n)}, t_{e(n)})$ in Eq. (22) – which means that, during the WTD process, there was some time point that led to the value of WP_n being equal to WD_n . Specifically, in the CP position, the $t_{c(n)}$ of *Spiraea pubescens* was longest (168.75 h), but, the soil water storage in *Andropogon* could

[Title Page](#)[Abstract](#)[Introduction](#)[Conclusions](#)[References](#)[Tables](#)[Figures](#)[Back](#)[Close](#)[Full Screen / Esc](#)[Printer-friendly Version](#)[Interactive Discussion](#)

reach its balance within 61.58 h (shortest). In the AP position, the $t_{c(n)}$ of the bare land cover was longest, and the soil moisture storage in *Artemisia coparia* ($t_{c(n)} = 121.17$ h) appeared to be faster to be on the $WP_n = WD_n$ condition than other two vegetated plots during the WTD processes.

5 4 Discussion

4.1 Spatiotemporal downscaling

Downscaling the spatiotemporal scale was based on integrating the CP/AP sampling schemes with the DTW/WTD hydrological processes (Fig. 10). The downscaled spatial scales of the CP/AP sampling scheme concentrated on the influence of the spatial structure diversity of the different land uses/cover in the Loess Plateau. Additionally, downscaling the temporal scales of the TSSM analysis through the classification of DTW and WTD was aimed to detail the fluctuation in the soil moisture over a short period triggered by precipitation and radiation, rather than focusing on the rainy season (Coppola et al., 2011; Heathman et al., 2012) or multiple-years (Biswas and Si, 2011; Brocca et al., 2010). Because the factors influencing soil moisture fluctuation were different in the two short processes, the main contributors affecting the dynamics of the soil moisture in the DTW process were infiltration, runoff and interception triggered by precipitation (Eagleson, 1978a, b), but the primary influential factor in the WTD process was radiation leading to evapotranspiration. Therefore, a finer spatiotemporal scale was the first step to try to understand the soil moisture dynamics based on the TSSM view, not just in the soil water content, although there were no significant differences among the 4 land uses/cover of different sampling positions.

4.2 Effect of hydrological processes on CP/AP sampling-based TSSM

The influence of the sampling scheme on the CP-TSSM or AP-TSSM in *Artemisia coparia* and *Spiraea pubescens* was more obvious than in the bare land cover and

[Title Page](#)

[Abstract](#)

[Introduction](#)

[Conclusions](#)

[References](#)

[Tables](#)

[Figures](#)



[◀](#)

[▶](#)

[Back](#)

[Close](#)

[Full Screen / Esc](#)

[Printer-friendly Version](#)

[Interactive Discussion](#)

Andropogon, which was related to the different spatial structures of the vertical direction between the two types. Specifically, three complex response components in both the DTW and WTD processes (Figs. 11 and 12) including the canopy being upon the ground, the litter layer covering the soil surface, and the root system being dispersed in the subsurface likely played different roles in the feedback of the different hydrological triggers and finally affected the CP/AP-TSSM of the different land uses/cover.

4.2.1 Influence of DTW processes on CP/AP-TSSM

The response of the main parameters of the CP/AP-TSSM to the DTW process, primarily triggered by precipitation is displayed in Fig. 11. The response units of the CP-TSSM of the vegetated plots were generally divided into three components. First, the stemflow (Levia and Frost, 2003; Li, 2011), set as a positive feedback for the soil water storage, may be the main water input at the CP position. Second, the point-based litter layer most likely restricted the water from migrating downward to the soil surface via the conservation or absorption action. Third, the infiltration zone in the base of the main root mainly formed preferential flow and removed the water from the surface layer (Li et al., 2009). The latter two response units may be considered to be the important water output factors of the surface layer, and regarded as negative feedbacks on water storage. Therefore, the dynamic balance state derived from the positive and negative feedbacks on the water storage of the soil surface reflected the characteristics of the CP-TSSM in *Artemisia scoparia* and *Spiraea pubescens*, and the diversity of morphological structure lead to the difference of the CP-TSSM between the two types of land uses during the DTW process. Specifically, *Spiraea pubescens* which has a more obvious stem structure to generate stemflow (Garcia-Estrinaga et al., 2010) than *Artemisia scoparia* was more beneficial to the formation of water input to CP position, which led to *Spiraea pubescens* having a higher soil moisture increment than *Artemisia scoparia* during the DTW process (Fig. 11).

With respect to the response units of AP-TSSM during the DTW process, *Artemisia scoparia* was also different from *Spiraea pubescens*. The water input of the AP

positions of the two vegetated land uses was primarily determined by the intermittent throughfall. Furthermore, other negative feedbacks on the water storage consisted of water conservation by the litter layer on the soil surface and the infiltration capacity of the soil subsurface. Therefore, the three response-unit variables to precipitation formed the function of the AP-TSSM and caused the divergence of the AP-TSSM between *Artemisia scoparia* and *Spiraea pubescens* land uses due to the different morphological characteristics. Specifically, the more expensive canopy structure of *Spiraea pubescens* most likely enabled it to have higher thresholds of interception (Lai et al., 2001) than *Artemisia scoparia* during precipitation, and also resulted in a higher increment of the soil moisture in the APs positions of *Artemisia scoparia*. Otherwise, in the bare plots and *Andropogon*, the potential negative feedbacks on the water storage in DTW processes – including a higher probability of occurrence of splash erosion and runoff – likely increased the complexity and uncertainty of their TSSM influential factors (Fig. 11).

4.2.2 Influence of WTD processes on CP/AP-TSSM

The contributors affecting the CP/AP-TSSM of the different land uses/cover in the WTD processes is showed in Fig. 12. In the hydrological processes, evapotranspiration was the fundamental pattern of the soil moisture loss, but especially in the vegetated plots, the complexity of the soil water movement in the root–soil interface (Caldwell et al., 1998; Dawson, 1993; Eagleson, 1978c; Horton and Hart, 1998; Porporato et al., 2002, 2001; Rodriguez-Iturbe et al., 2001) made it difficult to determine the specific response units of the soil water dynamics and also increased the uncertainty of the features of these response units. As a result, we only roughly divided the radiation response units of the CP/AP-TSSM in the vegetated land uses into three parts. Specifically, first, the litter lay in the CP/AP-TSSM played the role of restricting the water from being evaporated from the soil surface (Villegas et al., 2010), which could be determined as a negative feedback on the soil water losses; and secondly, the zones with a dispersion of main and lateral roots lost soil moisture through moisture absorption by the root

[Title Page](#)

[Abstract](#)

[Introduction](#)

[Conclusions](#)

[References](#)

[Tables](#)

[Figures](#)

◀

▶

◀

▶

[Back](#)

[Close](#)

[Full Screen / Esc](#)

[Printer-friendly Version](#)

[Interactive Discussion](#)

system; finally, the canopy being upon the ground acted as the main positive feedback on the soil water losses via transpiration. Meanwhile, different contributors existed that affected the CP-TSSM and AP-TSSM during these evapotranspiration processes. Primarily, the different amounts of water energy existing in the soil medium at the CP and AP positions would likely cause mutual transformation due to the changes in the dynamics between the soil water potential and the xylem osmotic (press) potential (Porporato et al., 2001) in the soil–plant interface system. Moreover, in the AP position, plant hydraulic lift (Li, 2011; Scholz et al., 2010) which may be regarded as negative feedback of water loss in the AP positions promotes water efflux from the roots of the plants into the soil layer passively when the transpiration action was under the reduced condition (Caldwell et al., 1998).

Admittedly, these complex water movement processes in the root–soil interface leads to the difficulty of interpreting the characteristics of the CP/AP-TSSM parameters of the vegetated plots, but the lower TSSM-MRD of the vegetated plots compared with the non-vegetated plots likely indicated that the canopy transpiration may have a stronger driving force to form a water output pattern than the evaporation of the bare soil surface, which, in the long term, indicates that the soil of vegetated land uses (*Artemisia scoparia* and *Spiraea pubescens*) was drier than that of the bare land cover in the Loess Plateau (Wang et al., 2013, 2012).

20 4.3 Implication of ET-TSSM's application on soil hydrological processes

In the ET-TSSM model, θ_S divides the WTD processes into three different stages. (1) From starting to $t_{s(n)}$, it demonstrated that the soil water content of the different land uses/cover decreased from the water profit condition based on the determination of θ_S ; (2) from $t_{s(n)}$ to $t_{c(n)}$, it represented that the soil moisture gradually reached the profit-deficit dynamic balance condition; (3) from $t_{c(n)}$ to $t_{e(n)}$, the soil moisture of all the plots finally on the net deficit situation. Although the soil moisture of the different land uses/cover showed no significant differences by the significant difference analysis, in the background of the TSSM, the parameters including WP_n , WD_n , $\Delta\theta_n$, $t_{s(n)}$, $t_{c(n)}$ in

Title Page

Abstract

Introduction

Conclusions

References

Tables

Figures

◀

▶

◀

▶

Back

Close

Full Screen / Esc

Printer-friendly Version

the ET-TSSM displayed obvious difference in both the CP and AP positions of 4 land uses/cover (Table 4), all of which most likely proved that the distinguishing temporal characteristics of the soil moisture existed at the finer spatiotemporal scales. Specifically, with respect to the CP sampling scheme, the higher $t_{c(n)}$ of *Spiraea pubescens* was influenced by the integration effect of hydraulic lift into the stemflow, both of which prolonged the time when the corresponding net deficit of the soil water content started to occur in the CP position. However, with respect to the AP positions, the higher $t_{c(n)}$ in the bare land cover would likely be related to the soil crust which was beneficial to the water infiltration (Bu et al., 2008; Eldridge and Greene, 1994; Eldridge and Rosenzreter, 1999) and may increased the temporal threshold of the emergence of the soil water net deficit condition.

Otherwise, from the view of the soil water balance, the lowest value of WD_n in the bare land cover and the lower value of $\Delta\theta_n$ in the vegetated land uses demonstrated that although all of plots' water contents were under the net deficit condition at the end of the WTD process ($\Delta\theta_n < 0$), the deficiency level of the soil moisture in the vegetated plots which have larger value of $|\Delta\theta_n|$ were significantly higher than the level of the bare land cover.

The results also suggested that the vegetated land uses which have a higher water consumption capacity by virtue of evapotranspiration processes would likely lead to a greater degree of soil water content storage reduction under radiation conditions (Wang et al., 2012), which could finally cause the formation of a drier layer in the Loess Plateau (Chen et al., 2010). This dryness has increasingly become a serious environmental problem after nearly 30 yr of the Grain for Green policy (Chen et al., 2008a, b; Shao et al., 2010). Therefore, from the TSSM view, the ET-TSSM model also suggested the importance of the efficient selection or management of plants during the process of vegetation restoration in the Loess Plateau, which has been considered a challenge to trade – off the effective prevention of soil erosion and reasonable utilization of available water resources in this water-controlled region.

Temporal stability of soil moisture under different land uses/cover

J. Zhou et al.

[Title Page](#)

[Abstract](#)

[Introduction](#)

[Conclusions](#)

[References](#)

[Tables](#)

[Figures](#)



[Back](#)

[Close](#)

[Full Screen / Esc](#)

[Printer-friendly Version](#)

[Interactive Discussion](#)

4.4 Uncertainties and limitation

First, we admit that the CP/AP sampling scheme could lead to system errors, a number of which may decrease the accuracy of the TSSM calculation and fit of the ET-TSSM models. From long-term perspective, the installment of a fixed soil-moisture-measuring tube (Jost et al., 2012) in different plots appeared to be an efficient method to reduce the errors. However, the higher cost of the corresponding instrument needed to optimize the number of sampling points, and the more intensive disturbance to the soil profile during the mounting process most likely introduced new errors at the beginning of the soil moisture measurements. Second, as an empirical model, the ET-TSSM model was based on collected data rather than on some physical law. Therefore, some derived parameters of the model were unable to interpret all the soil moisture dynamics in the hydrological processes, such as the uncertainties of the dimensions of WP_n and WD_n , which both only reflect the accumulation effect of the soil water content on different duration time via an integral expression (Eqs. 17 and 19). Finally, whether the TSSM-based model could be expanded to the DTW process is uncertain. The observation that the soil water content of different land uses increased notably sharply over a short time (Heathman et al., 2012) in the DTW process could make it difficult to collect the data in an artificial manner, which is why we only constructed the ET-TSSM model using the WTD process. As a result, it was also necessary to introduce an automatic soil moisture logger system (Wang et al., 2012) to assist the TSSM research in the WTD process when the study spatiotemporal scale was downscaled.

5 Conclusions

In this study, we analyzed the characteristics of the TSSM in different land uses/cover under a finer spatiotemporal scale, and first introduced the TSSM concept into hydrological processes by the application of the ET-TSSM model. In the DTW process, the difference in the TSSM between the CP/AP positions of vegetated land uses was

Title Page	
Abstract	Introduction
Conclusions	References
Tables	Figures
	
	
Back	Close
Full Screen / Esc	
Printer-friendly Version	
Interactive Discussion	

related to the diversity of plant morphological structures upon the ground, which affected the water input pattern of precipitation. However, in the WTD process, the difference could most likely be ascribed to the diversity of transpiration derived from various canopy structures and the complexity of water movement existing in the root–soil interface. From the TSSM view, the parameters of the ET-TSSM model indicated that vegetated land uses more easily affected the net deficit condition than the bare land cover during the WTD process, which likely cause the soil to become drier when there was a lack of reasonable vegetation selections in the Loess Plateau. However, due to the error derived from the CP/AP sampling scheme and the limitation of the ET-TSSM model to interpret the hydrological processes, future studies needed to further improve the accuracy of the sampling and to modify certain parameters of the ET-TSSM model.

Acknowledgements. This work was funded by the National Natural Science Foundation of China (No. 41230745 and 41101096) and the CAS/SAFEA International Partnership Program for Creative Research Teams of “Ecosystem Processes and Services”.

15 References

- Biswas, A. and Si, B. C.: Scales and locations of time stability of soil water storage in a hummocky landscape, *J. Hydrol.*, 408, 100–112, 2011.
- Brocca, L., Morbidelli, R., Melone, F., and Moramarco, T.: Soil moisture spatial variability in experimental areas of central Italy, *J. Hydrol.*, 333, 356–373, 2007.
- 20 Brocca, L., Melone, F., Moramarco, T., and Morbidelli, R.: Soil moisture temporal stability over experimental areas in Central Italy, *Geoderma*, 148, 364–374, 2009.
- Brocca, L., Melone, F., Moramarco, T., and Morbidelli, R.: Spatial-temporal variability of soil moisture and its estimation across scales, *Water Resour. Res.*, 46, W02516, doi:10.1029/2009WR008016, 2010.
- 25 Bu, C. F., Cai, Q. G., Zhang, X. C., and Ma, L.: Review on developmental characteristics and ecological functions of soil crust, *Prog. Geogr.*, 27, 26–31, 2008 (in Chinese).
- Caldwell, M. M., Dawson, T. E., and Richard, J. H.: Hydraulic lift: consequences of water efflux from the roots of plants, *Oecologia*, 113, 151–161, 1998.

[Title Page](#)[Abstract](#)[Introduction](#)[Conclusions](#)[References](#)[Tables](#)[Figures](#)[Back](#)[Close](#)[Full Screen / Esc](#)[Printer-friendly Version](#)[Interactive Discussion](#)

- Chen, H. S., Shao, M. A., and Li, Y. Y.: Soil desiccation in the Loess Plateau of China, *Geoderma*, 143, 91–100, 2008a.
- Chen, H. S., Shao, M. A., and Li, Y. Y.: The characteristics of soil water cycle and water balance on steep grassland under natural and simulated rainfall conditions in the Loess Plateau of China, *J. Hydrol.*, 360, 242–251, 2008b.
- Chen, L. D., Wang, J. P., Wei, W., Fu, B. J., and Wu, D. P.: Effects of landscape restoration on soil water storage and water use in the Loess Plateau Region, China, *Forest Ecol. Manag.*, 259, 1291–1298, 2010.
- Coppola, A., Comegna, A., Dragonetti, G., Lamaddalena, N., Kader, A. M., and Comegna, V.: Average moisture saturation effects on temporal stability of soil water spatial distribution at field scale, *Soil Till. Res.*, 114, 155–164, 2011.
- Cosh, M. H., Jackson, T. J., Starks, P., and Heathman, G.: Temporal stability of surface soil moisture in the Little Washita River watershed and its applications in satellite soil moisture product validation, *J. Hydrol.*, 323, 168–177, 2006.
- Dawson, T. E.: Hydraulic lift and water use by plants: implication for water balance performance and plant-plant interaction, *Oecologia*, 95, 565–574, 1993.
- Eagleson, P. S.: Climate, soil and vegetation 1. Introduction to water balance dynamics, *Water Resour. Res.*, 14, 705–712, 1978a.
- Eagleson, P. S.: Climate, soil and vegetation 2. The distribution of annual precipitation derived from observed storm sequences, *Water Resour. Res.*, 14, 713–721, 1978b.
- Eagleson, P. S.: Climate, soil and vegetation 4. The expected value of annual evapotranspiration, *Water Resour. Res.*, 14, 731–739, 1978c.
- Eldridge, D. J. and Greene, R. S. B.: Microbiotic soil crust: a review of their roles in soil and ecological processes in rangeland of Australia, *Austr. J. Soil Res.*, 32, 389–415, 1994.
- Eldridge, D. J. and Rosentreter, R.: Morphological groups: a framework for monitoring microphytic crusts in arid landscapes, *J. Arid Environ.*, 41, 11–25, 1999.
- Gao, G. Y., Fu, B. J., Lü, Y. H., Liu, Y., Wang, S., and Zhou, J.: Coupling the modified SCS-CN and RUSLE models to simulate hydrological effects of restoring vegetation in the Loess Plateau of China, *Hydrol. Earth Syst. Sci.*, 16, 2347–2364, doi:10.5194/hess-16-2347-2012, 2012.
- Gao, L. and Shao, M. A.: Temporal stability of soil water storage in diverse soil layers, *Catena*, 95, 24–32, 2012.

Temporal stability of soil moisture under different land uses/cover

J. Zhou et al.

[Title Page](#)

[Abstract](#)

[Introduction](#)

[Conclusions](#)

[References](#)

[Tables](#)

[Figures](#)



[Back](#)

[Close](#)

[Full Screen / Esc](#)

[Printer-friendly Version](#)

[Interactive Discussion](#)

- Gao, X. D., Wu, P. T., Zhao, X. N., Shi., Y. G., Wang, J. W., and Zhang, B. Q.: Soil moisture variability along transects over a well-developed gully in the Loess Plateau, China, *Catena*, 87, 357–367, 2011.
- 5 Garcia-Estringana, P., Alonso-Blázquez, N., and Alegre, J.: Water storage capacity, stemflow and water funneling in Mediterranean shrubs, *J. Hydrol.*, 389, 363–372, 2010.
- Heathman, G. C., Cosh, M. H., Han, E., Jackson, T. J., McKee, L., and McAfee, S.: Field scale spatiotemporal analysis of surface soil moisture for evaluating point-scale in situ networks, *Geoderma*, 170, 195–205, 2012.
- Horton, J. L. and Hart, S. C.: Hydraulic lift: a potentially important ecosystem process, *Trends Ecol. Evol.*, 13, 232–235, 1998.
- 10 Hu, W., Shao, M. A., Han, F. P., Reichardt, K., and Tan, J.: Watershed scale temporal stability of soil water content, *Geoderma*, 158, 181–198, 2010.
- Jacobs, J. M., Mohanty, B. P., Hsu, E., and Miller, D.: SMEX02: field scale variability, time stability and similarity of soil moisture, *Remote Sens. Environ.*, 92, 436–446, 2004.
- 15 Jia, Y. H. and Shao, M. A.: Temporal stability of soil water storage under four types of revegetation on the northern Loess Plateau of China, *Agr. Water Manage.*, 117, 33–42, 2013.
- Jost, G., Schume, H., Hager, H., Markart, G., and Kohl, B.: A hillslope scale comparison of tree species influence on soil moisture dynamics and runoff processes during intense rainfall, *J. Hydrol.*, 420–421, 112–124, 2012.
- 20 Laio, F., Porporato, A., Ridolfi, L., and Rodriguez-Iturbe, I.: Plant in water-controlled ecosystems active role in hydrologic processes and response to water stress, II. Probabilistic soil moisture dynamics, *Adv. Water Resour.*, 24, 707–723, 2001.
- Levia, D. F. and Frost, E. E.: A review and evaluation of stemflow literature in the hydrologic and biogeochemical cycles of forested and agricultural, *J. Hydrol.*, 274, 1–29, 2003.
- 25 Li, X. Y.: Mechanism of coupling, response and adaptation between soil, vegetation and hydrology in arid and semiarid regions, *Sci. China Ser. D*, 41, 1721–1730, 2011 (in Chinese).
- Li, X.-Y., Yang, Z.-P., Li, Y.-T., and Lin, H.: Connecting ecohydrology and hydropedology in desert shrubs: stemflow as a source of preferential flow in soils, *Hydrol. Earth Syst. Sci.*, 13, 1133–1144, doi:10.5194/hess-13-1133-2009, 2009.
- 30 Li, Y., Poesen, J., Yang, J. C., Fu, B., and Zhang, J. H.: Evaluating gully erosion using ^{137}Cs and $^{210}\text{Pb}/^{137}\text{Cs}$ ratio in a reservoir catchment, *Soil Till. Res.*, 69, 107–115, 2003.

[Title Page](#)[Abstract](#)[Introduction](#)[Conclusions](#)[References](#)[Tables](#)[Figures](#)[Back](#)[Close](#)[Full Screen / Esc](#)[Printer-friendly Version](#)[Interactive Discussion](#)

Temporal stability of soil moisture under different land uses/cover

J. Zhou et al.

[Title Page](#)[Abstract](#)[Introduction](#)[Conclusions](#)[References](#)[Tables](#)[Figures](#)[Back](#)[Close](#)[Full Screen / Esc](#)[Printer-friendly Version](#)[Interactive Discussion](#)

- Tian, J. L. and Peng, X. L.: Geochemistry of Soil in the Loess Plateau, Science press, Beijing, 1994 (in Chinese).
- Vachaud, G., Passerat De Silans, A., Balabanis, P., and Vauclin, M.: Temporal stability of spatially measured soil water probability density function, *Soil Sci. Soc. Am. J.*, 49, 822–828, 1985.
- Van Pelt, R. S. and Wierenga, P. J.: Temporal stability of spatially measured soil water matric potential probability density, *Soil Sci. Soc. Am. J.*, 65, 668–667, 2001.
- Villegas, J. C., Breshears, D. D., Zou, C. B., and Law, D. J.: Ecohydrological controls of soil evaporation in deciduous drylands: how the hierarchical effects of litter, patch and vegetation mosaic cover interact with phenology and season, *J. Arid Environ.*, 74, 595–602, 2010.
- Wang, S., Fu, B. J., Gao, G. Y., Yao, X. L., and Zhou, J.: Soil moisture and evapotranspiration of different land cover types in the Loess Plateau, China, *Hydrol. Earth Syst. Sci.*, 16, 2883–2892, doi:10.5194/hess-16-2883-2012, 2012.
- Wang, S., Fu, B. J., Gao, G. Y., Liu, Y., and Zhou, J.: Responses of soil moisture in different land cover types to rainfall events in a re-vegetation catchment area of the Loess Plateau, China, *Catena*, 101, 122–128, 2013.
- Wang, Y. F., Fu, B. J., Chen, L. D., Lü, Y. H., and Luo, C. Y.: Effects of land use change on soil erosion intensity in small watershed of Loess Hilly Region: a quantitative evaluation with ¹³⁷Cesium tracer, *Chinese J. Appl. Ecol.*, 20, 1571–1576, 2009 (in Chinese).

Discussion Paper | Discussion Paper

Temporal stability of soil moisture under different land uses/cover

J. Zhou et al.

[Title Page](#)[Abstract](#)[Introduction](#)[Conclusions](#)[References](#)[Tables](#)[Figures](#)[Back](#)[Close](#)[Full Screen / Esc](#)[Printer-friendly Version](#)[Interactive Discussion](#)

Temporal stability of soil moisture under different land uses/cover

J. Zhou et al.

Table 1. Characteristics of four land uses/cover in Yangjuangou catchment.

Land Uses/Cover	Plot Code	Physical Characteristics				Morphological Characteristics				
		Clay %	Silt %	Sand %	BD g cm ⁻³ ^a	H cm ^b	LS cm ^c	C cm ^d	Coverage %	Slope (%)
Bare	Plot1	9.21 ± 1.21	26.04 ± 2.41	64.75 ± 1.85	1.24 ± 0.09	0	0	0	0	26.8
Andropogon	Plot2	8.48 ± 2.14	25.28 ± 1.98	66.24 ± 2.24	1.26 ± 0.11	20 ~ 30	0	0	70 ~ 85	26.8
Artemisia coparia	Plot3	9.54 ± 1.48	26.72 ± 2.87	63.74 ± 3.24	1.13 ± 0.10	45 ~ 55	0	60 ~ 70	95 ~ 100	26.8
Spiraea pubescens	Plot4	11.98 ± 3.15	22.24 ± 3.84	65.78 ± 4.51	1.21 ± 0.08	120 ~ 150	40 ~ 50	70 ~ 100	100	26.8

^a Soil bulk density.

^b Average height of vegetated land uses.

^c Average Length of stem only owned by *Spiraea pubescens*.

^d Average Crown width.

Title Page

Abstract

Introduction

Conclusions

References

Tables

Figures

◀

▶

◀

▶

Back

Close

Full Screen / Esc

Printer-friendly Version

Interactive Discussion

Table 2. Main characteristics of TSSM parameters in hydrological processes.

^a SS	Plot Code	Hydrological Processes				WTD Processes			
		CumuP ($\theta_{CP[k]}$)	^c OEM $\bar{\delta}_j > 0$	^d UEM $\bar{\delta}_j < 0$	$\varsigma(\bar{\delta}_j)$	CumuP ($\theta_{CP[k]}$)	OEM $\bar{\delta}_j > 0$	UEM $\bar{\delta}_j < 0$	$\varsigma(\bar{\delta}_j)$
CP	Plot1	x	(2)(3)(4)	(1)	0.09	^e x	(1)(2)(3)(4)	x	0.08
	Plot2	^b (4)/0.47	(1)	(1)(2)(3)	0.15	(2)/0.47	(2)	(1)(3)(4)	0.09
	Plot3	x	(1)	(2)(3)(4)	0.08	(1)/0.53	(1)	(2)(3)(4)	0.04
	Plot4	(2)/0.53	(1)	(2)(3)(4)	0.13	x	(1)(4)	(2)(3)	0.16
AP	Plot1	(1)/0.46	(1)(2)(3)(4)	x	0.05	x	(1)(2)(3)(4)	x	0.07
	Plot2	x	(1)(2)	(3)(4)	0.08	(1)/0.48, (1)/0.54	(1)	(2)(3)(4)	0.12
	Plot3	(1)/0.53	(1)(2)(3)(4)	x	0.09	x	x	(1)(2)(3)(4)	0.10
	Plot4	x	(1)	(2)(3)(4)	0.08	x	x	(1)(2)(3)(4)	0.10

^a Sampling Scheme.^b means the cumulative probability of soil moisture in Plot2(1) was 0.47 in the DTW processes.^c Overestimation.^d Underestimation.^e means no plot meet the corresponding condition of the MRD and cumulative probability.[Title Page](#)[Abstract](#)[Introduction](#)[Conclusions](#)[References](#)[Tables](#)[Figures](#)[Full Screen / Esc](#)[Printer-friendly Version](#)[Interactive Discussion](#)

Temporal stability of soil moisture under different land uses/cover

J. Zhou et al.

Table 3. Selection of parameter of TSSM in ET-TSSM model. The bold data representing the statistical parameters of Plot4(3) and Plot3(2) respectively, were selected as the main parameters of ET-TSSM model application during different hydrological processes.

DTW to WTD Processes							
SS	Plot Code	^a Similar Rank CumuP	Same Rank MRD	CumuP ($\theta_{CP(k)}$) ^b DTW/WTD	MDR ($\bar{\delta}_j$) ^c DTW/WTD	STD $\zeta(\bar{\delta}_j)$ ^d DTW/WTD	θ_S
CP	Plot1	(4)	(4)	0.86/0.86	0.081/0.091	0.073/0.074	Plot4 (3)
	Plot2	x	x	x	x	x	
	Plot3	x	x	x	x	x	
	Plot4	(1) (3)	(1) (3)	0.93/0.93 0.59/0.59	0.125/0.101 -0.034/ -0.004	0.045/0.115 0.200/0.129	
AP	Plot1	(2) (3)	(2) (3)	0.93/1.00 0.86/0.93	0.115/0.120 0.085/0.114	0.068/0.053 0.032/0.066	Plot3 (2)
	Plot2	x	x	x	x	x	
	Plot3	(2)	(2)	0.66/0.67	0.040/ - 0.005	0.028/0.055	
	Plot4	(3) (4)	(3) (4)	0.79/0.79 0.34/0.42	0.043/-0.014 0.005/-0.042	0.188/0.141 0.076/0.071	

^a means the difference between cumulative probability of the same land uses/cover in WTD and DTW processes was less than 0.1, which was also indicated $\Delta \text{CumuP}(\theta_{CP(k)}) < 0.1$.

^b means the specific cumulative probability value in WTD and DTW processes which have the similar rank cumulative probability.

^c means the specific mean relative difference values of soil moisture in WTD and DTW processes which have the same rank about mean relative difference.

^d means the specific deviation of average soil moisture in WTD and DTW processes which the same rank about mean relative difference.

- [Title Page](#)
- [Abstract](#) [Introduction](#)
- [Conclusions](#) [References](#)
- [Tables](#) [Figures](#)
- [◀](#) [▶](#)
- [◀](#) [▶](#)
- [Back](#) [Close](#)
- [Full Screen / Esc](#)
- [Printer-friendly Version](#)
- [Interactive Discussion](#)

Table 4. Characteristics of parameters derived from ET-TSSM model.

SS	Plot Code	$\theta_n(t)$	R^2	$t_{s(n)}$ h	$t_{c(n)}$ h	$\theta_{c(n)}$ %	WP _n	WD _n	$\Delta\theta_n$
CP θ_s = 16.6 %	Plot1	$\theta_1(t) = 12.78 + 13.61 \times 0.976^t$	0.948	52.30	142.01	13.21	203.21	743.63	-540.42
	Plot2	$\theta_2(t) = 11.67 + 10.20 \times 0.973^t$	0.897	26.56	61.58	13.56	61.58	1108.91	-1047.33
	Plot3	$\theta_3(t) = 10.39 + 12.72 \times 0.984^t$	0.942	44.45	102.80	12.81	127.55	1134.98	-1007.43
	Plot4	$\theta_4(t) = 8.15 + 17.55 \times 0.990^t$	0.918	72.72	168.75	11.37	290.93	1074.94	-784.01
AP θ_s = 16.4 %	Plot1	$\theta_1(t) = 11.89 + 14.73 \times 0.984^t$	0.942	73.38	193.57	12.54	302.68	697.09	-394.41
	Plot2	$\theta_2(t) = 1.95 + 12.06 \times 0.986^t$	0.877	56.34	132.83	12.80	161.80	890.76	-728.96
	Plot3	$\theta_3(t) = 10.36 + 14.56 \times 0.983^t$	0.931	51.32	121.17	12.12	186.96	1083.39	-896.43
	Plot4	$\theta_4(t) = 7.34 + 14.53 \times 0.993^t$	0.929	67.24	147.03	12.51	169.48	983.86	-814.38

Temporal stability of soil moisture under different land uses/cover

J. Zhou et al.

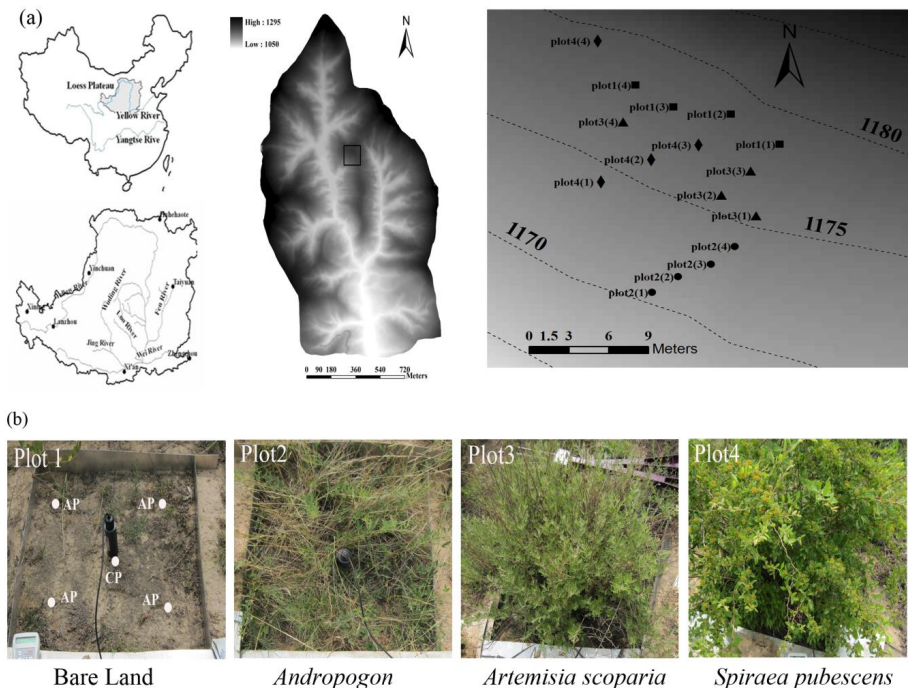


Fig. 1. Description of research area and CP/AP sampling scheme. **(a)** study area, **(b)** different land uses/cover. The black square, round, triangle and diamond dispersing topographic map represent the bare land cover (plot1), *Andropogon* (plot2), *Artemisia coparia* (plot3), and *Spiraea pubescens* (plot4) respectively. For each land uses/cover type, there are four microplots whose code was displayed in parentheses. Every microplot ($60\text{ cm} \times 60\text{ cm}$) was fenced by PVC sheets which were installed in the soil and 30 cm above the ground. CP and AP show the locations of soil moisture sampling, and we carefully mend the disturbance of soil surface layer after completion of each measurement by TDR.

10114

Temporal stability of soil moisture under different land uses/cover

J. Zhou et al.

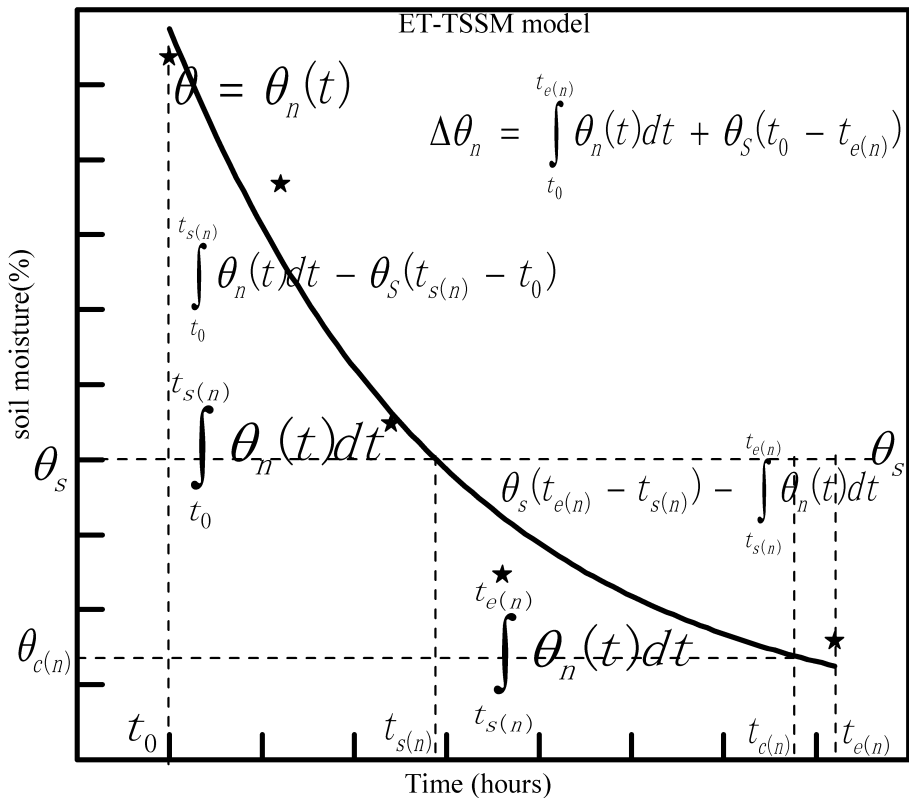


Fig. 2. Framework of ET-TSSM model and its parameters, supposed soil moisture values were represented by star marks fitting the ET curve. main parameters of ET-TSSM were explained in method. The area surround by ET curve, vertical line of t_0 and $t_{s(n)}$ as well as horizontal line of θ_S indicates the WP_n, and the other area surround by ET curve, vertical line of $t_{e(n)}$ and $t_{s(n)}$, horizontal line of θ_S represent the WD_n.

Temporal stability of soil moisture under different land uses/cover

J. Zhou et al.

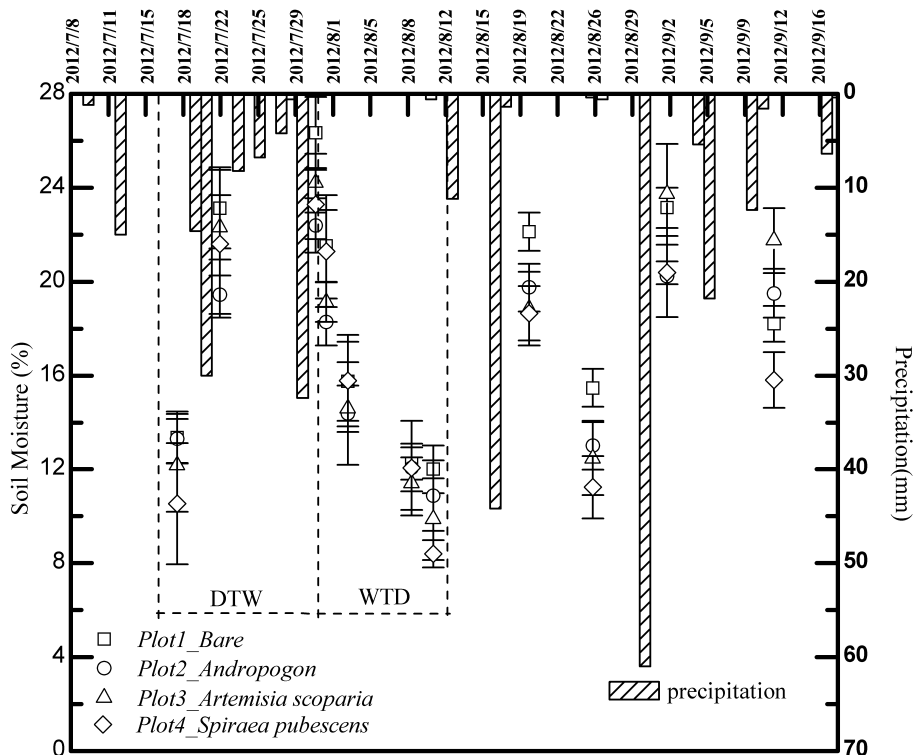


Fig. 3. Response of soil moisture to precipitation and radiation in rainy season of 2012. DTW and WTD represent the selected two hydrological processes triggered by precipitation and radiation respectively.

Temporal stability of soil moisture under different land uses/cover

J. Zhou et al.

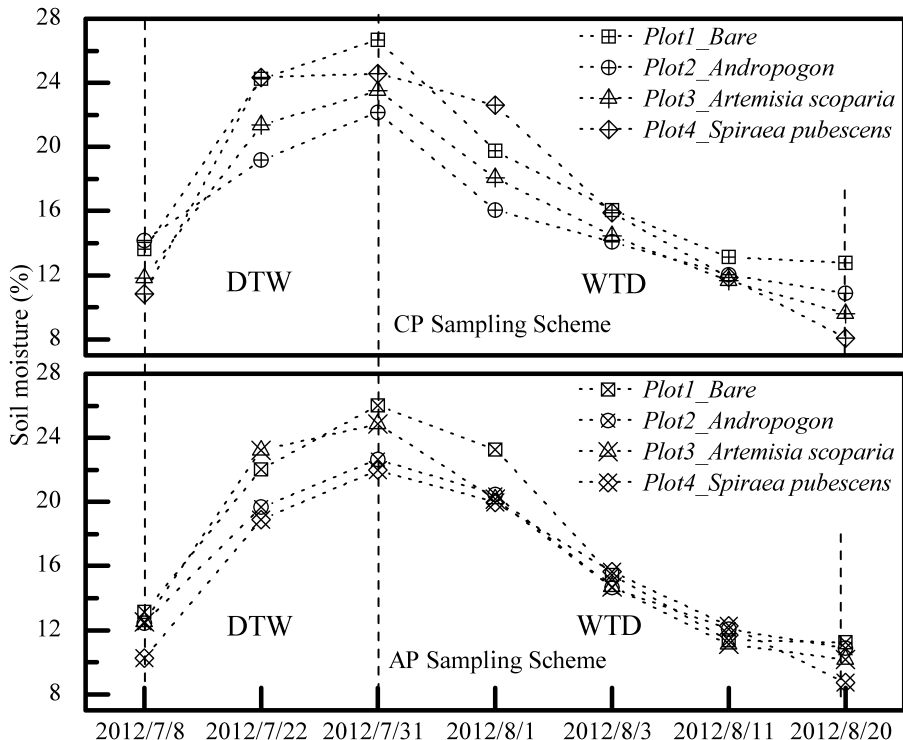


Fig. 4. Response of soil moisture to Hydrological processes based on CP/AP sampling schemes. In WTD and DTW processes, the soil moisture of four different land uses/cover at the same sampling position showed no significant difference ($P < 0.05$), and the soil moisture in the same land uses/cover at two different sampling position was also no significant difference ($P < 0.05$ for T test).

Temporal stability of soil moisture under different land uses/cover

J. Zhou et al.

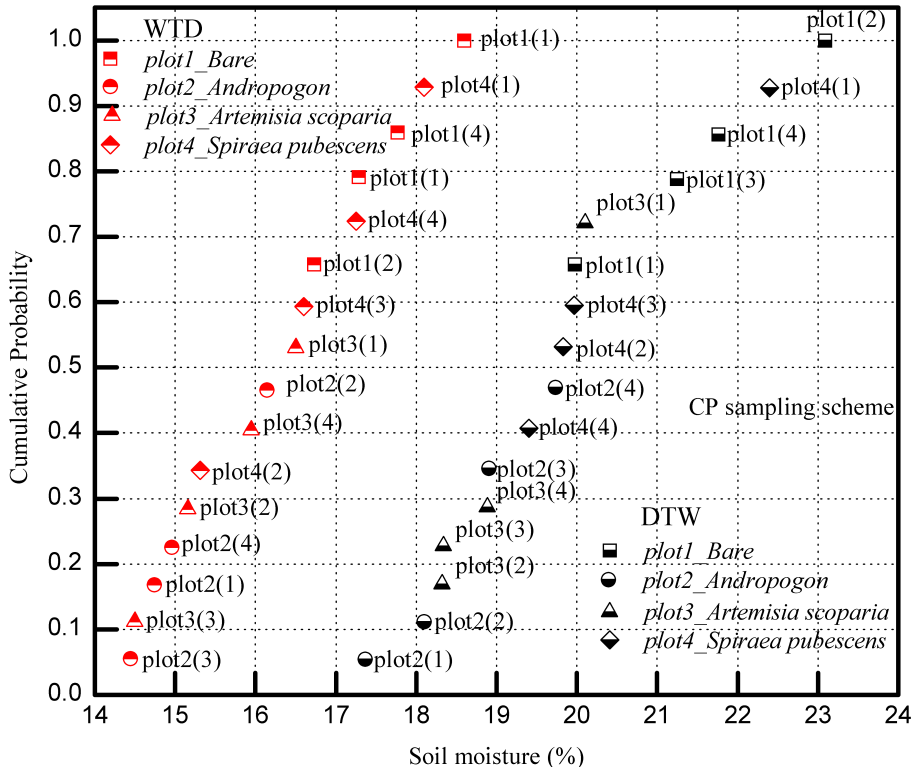


Fig. 5. Cumulative probability of soil moisture in hydrological processes based on CP sampling scheme, the red marks illuminate the cumulative probability distribution of average soil moisture in different land uses/cover over WTD process, and the black marks represent the cumulative probability distribution over DTW processes.

Temporal stability of soil moisture under different land uses/cover

J. Zhou et al.

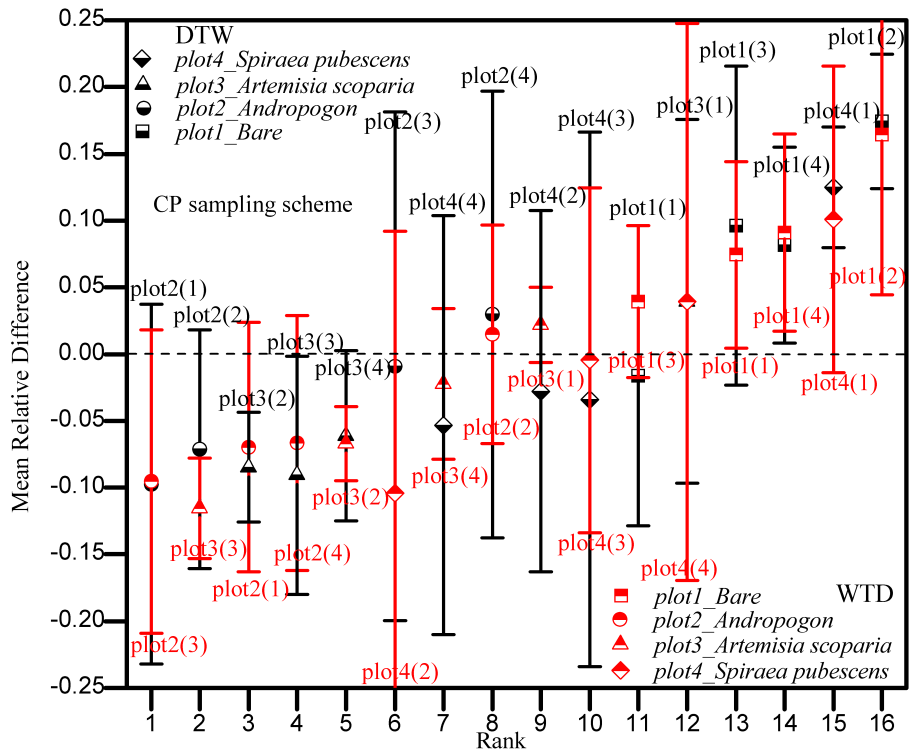


Fig. 6. Mean relative difference of soil moisture in hydrological processes based on CP sampling scheme, the red marks and error bar indicate the mean relative difference and deviation of different land uses/cover respectively over DTW processes, and the black marks and error bar represent mean relative difference and deviation over WTD processes.

Temporal stability of soil moisture under different land uses/cover

J. Zhou et al.

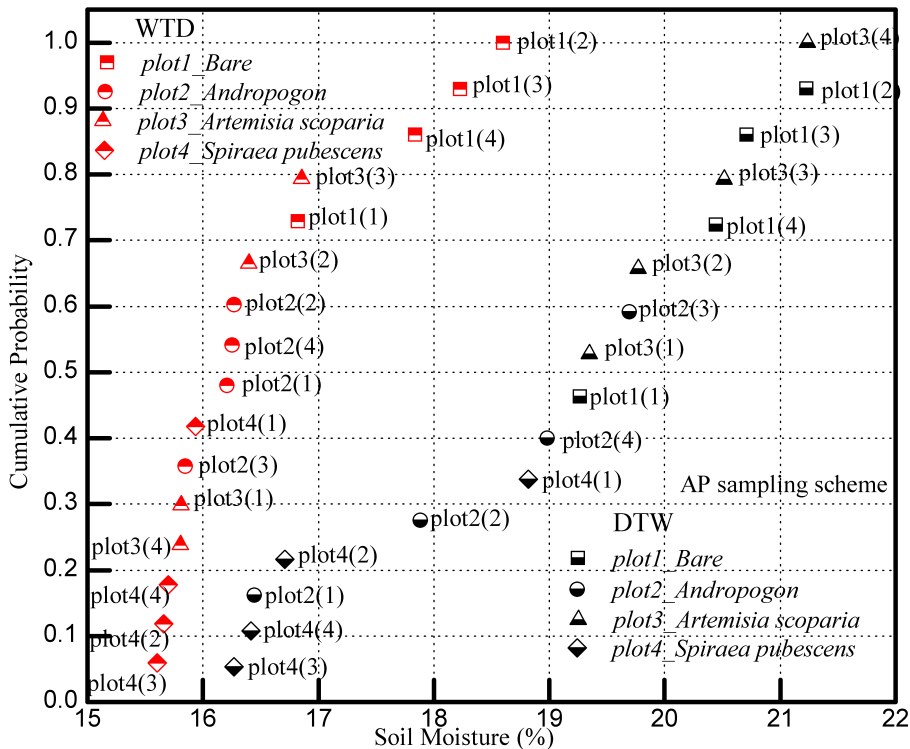


Fig. 7. Cumulative probability of soil moisture in hydrological processes based on AP sampling scheme, the red marks illuminate the cumulative probability distribution of average soil moisture in different land uses/cover over WTD process, and the black marks represent the cumulative probability distribution over DTW processes.

[Title Page](#)[Abstract](#)[Introduction](#)[Conclusions](#)[References](#)[Tables](#)[Figures](#)[Full Screen / Esc](#)[Printer-friendly Version](#)[Interactive Discussion](#)

Temporal stability of soil moisture under different land uses/cover

J. Zhou et al.

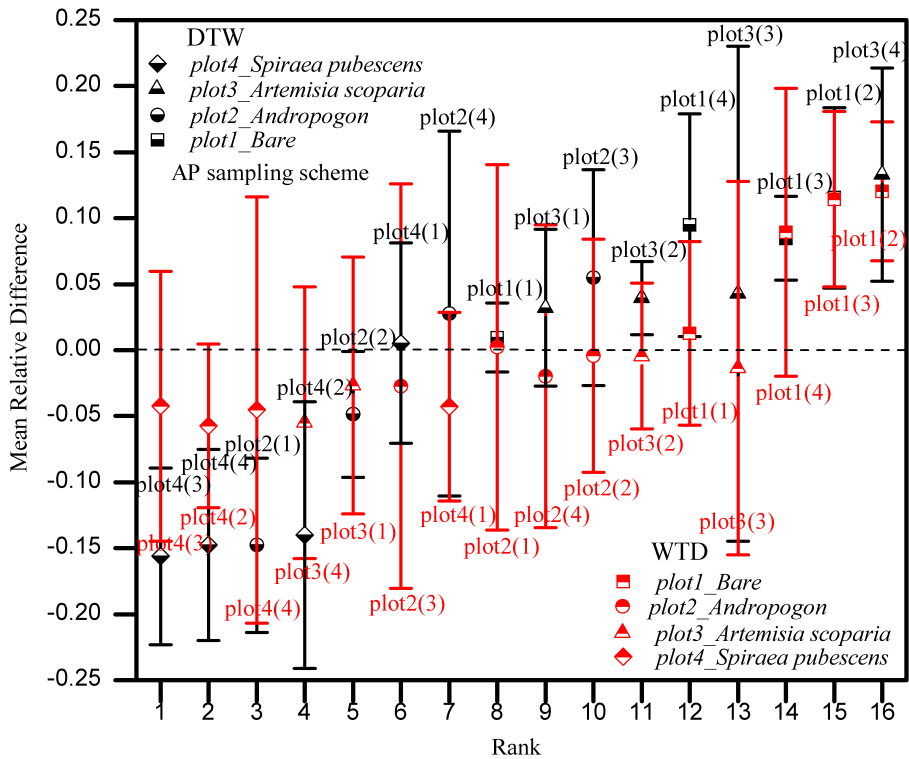


Fig. 8. Mean relative difference of soil moisture in hydrological processes based on AP sampling scheme, the red marks and error bar indicate the mean relative difference and deviation of different land uses/cover respectively over DTW processes, and the black marks and error bar represent mean relative difference and deviation over WTD processes.

Temporal stability of soil moisture under different land uses/cover

J. Zhou et al.

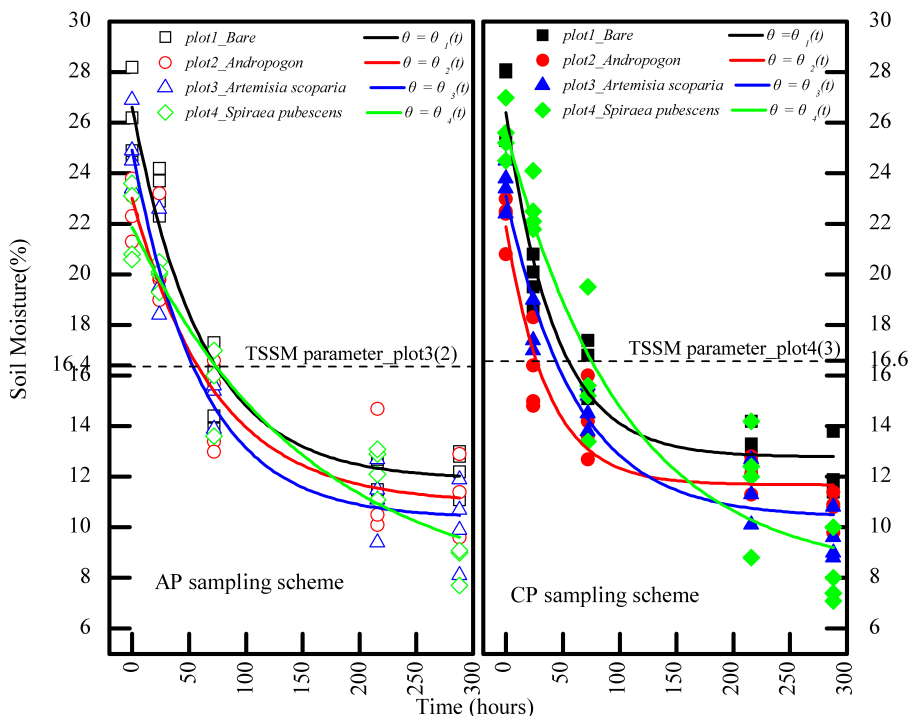


Fig. 9. Application of ET-TSSM model on hydrological processes based on CP/AP sampling schemes. The dash line in the left and right indicate the average moisture of *Artemisia scoparia* land use and *Spiraea pubescens* over WTD processes respectively.

Temporal stability of soil moisture under different land uses/cover

J. Zhou et al.

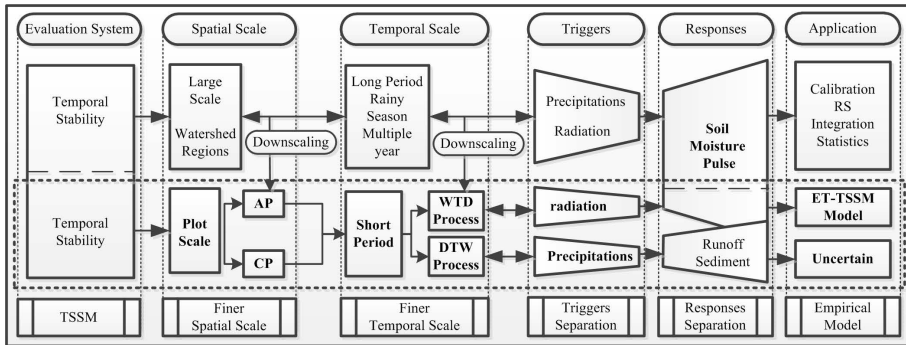


Fig. 10. Framework of finer spatiotemporal scales of TSSM research, the figures in thick dash box displays the specific method of spatiotemporal downscaling and hydrological response separation. And the “uncertain box” means the uncertain whether the TSSM-based model could be expanded on DTW processes which could be the future study on the application of TSSM in finer spatiotemporal scale.

Temporal stability of soil moisture under different land uses/cover

J. Zhou et al.

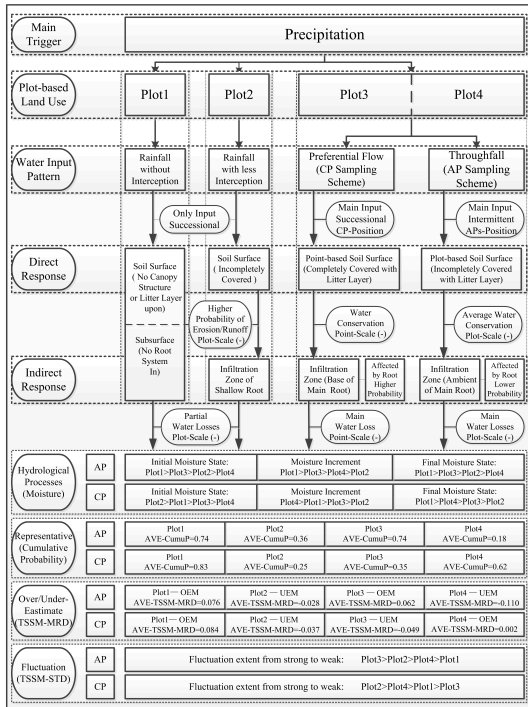


Fig. 11. Influence of hydrological processes on TSSM parameter over DTW period. The whole hydrological processes was divided three parts, including water input pattern, direct response and indirect response. And the solid arrow represents the approximate direction of soil moisture movement in the plant-soil environment. The minus sign in box means that the corresponding response was the negative feedback on the water increment, and the plus sign in box indicates the corresponding responses which probably improve the water input to the soil matrix and lead to the soil water increment.

Temporal stability of soil moisture under different land uses/cover

J. Zhou et al.

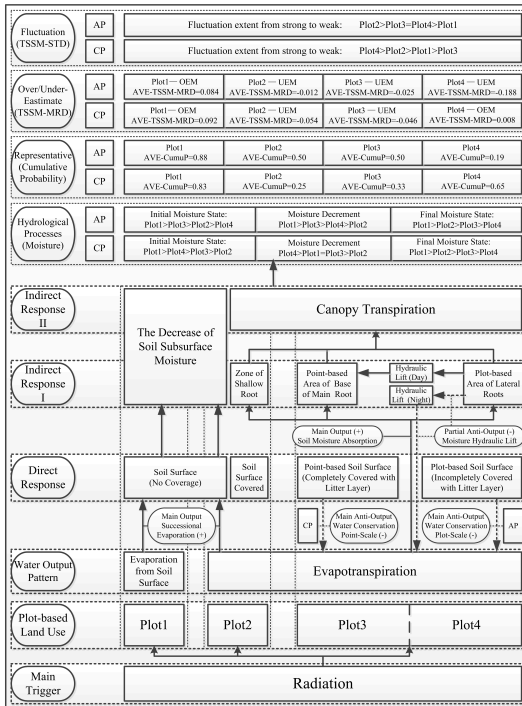


Fig. 12. Influence of hydrological processes on TSSM parameter over WTD period. Water output pattern, direct response and two indirect responses constitutes the hydrological processes, solid arrow represents the approximate direction of soil moisture coming out from the plant or soil systems, and the dash arrow shows the direction of soil moisture movement to enter the soil matrix. And minus sign in box means that the corresponding response restricting the soil moisture from evapotranspirating the soil-plant environment, and the plus sign in box indicates the corresponding responses which was the positive feedback on the water output leading to the soil water decrease.